Stable Orbit of Massive Klein Gordon Field near Schwarzschild Black Hole and Its Quasi-Normal Modes

Pradip Sharma*

Tribhuvan University, Nepal

*Corresponding Author
Pradip Sharma, Tribhuvan University, Nepal.

Abstract
The findings of bound states of the massive Klein-Gordon field near the Schwarzschild black hole have provided certain conditions for a stable orbit. Unlike classical methods, I have obtained a specific relation between the mass of the scalar particle and the distance from the black hole. Furthermore, by applying a polynomial condition to the Heun function, more accurate predictions of quasi-normal modes have been made. Based on this, the time of a stable orbit and its relationship with mass, polynomial order, and distance from the Schwarzschild black hole have been calculated.

1. Introduction

In the scientific exploration of the Schwarzschild black hole, researchers have investigated the dynamics of particles through classical methods. These investigations have encompassed the stability of objects and the range of distances from the event horizon that allow for stable orbits in its vicinity. Additionally, the scattering behavior of particles moving away from or towards the black hole has been calculated. By utilizing the wave equation approach, researchers have obtained dynamic solutions for objects and quasi-normal modes. The results have shown a high level of accuracy when compared to experimental methods.

During these findings, implementing a quantum mechanical approach in the presence of strong gravity posed challenges. Therefore, the focus of research shifted towards quantum field theory in curved spacetime, specifically in the vicinity of strong gravity. Scientists explored the nature of incoming and outgoing waves for massless particles through scattering theory. The complex nature of quasi-normal modes with different spins provided insight into the stability of waves near strong gravity, and many researchers employed various approaches to calculate this. Furthermore, scientists formulated the behavior of massive Klein-Gordon (KG) fields near Schwarzschild and Kerr black holes. Despite the extensive research conducted during that time, satisfactory results were seldom achieved due to the influence of singularity near the black hole. To address this issue, the mathematical formulation of the Heun function was introduced, which helped alleviate the problem of singularity in the dynamics of particles and waves near the black hole to some extent. Leveraging the properties of the Heun function, the bound states of massive and massless particles were presented with greater accuracy compared to previous methods. Quasi-normal modes, including the value and effect of the imaginary part of energy, were accurately explained. Some papers explored the polynomial conditions of the Heun function, yielding peculiar results. Despite the substantial amount of work in this field, the dependence of the stability of scalar particles near the Schwarzschild black hole on mass remains unknown. Additionally, the variation in the nature of stable orbits with distance from the event horizon for massive particles are rarely studied. The effect of employing polynomial conditions of the Heun function on the wave function for the Klein-Gordon equation is still uncertain. Furthermore, calculating the relationship between the quasi-normal modes, the polynomial order, and mass presents difficulties. Lastly, the nature of stability of the orbit and its dependence on mass and the imaginary part of energy is a significant challenge.

The focus of my work revolves around addressing the unresolved issues mentioned in the previous paragraph. In the first section, I calculate the potential energy using the tortoise coordinate system for the Klein-Gordon equation in the Schwarzschild black hole [1-10]. Furthermore, I present the minimum distance from the event horizon required for a stable orbit. I also include the maximum mass for orbital motion and variations of mass with distance for different values of orbital momentum in this section. The second section focuses on determining the energy of quasi-normal modes for different values of the polynomial order of the Confluent Heun function (HeunC). Additionally, I establish the relationship between complex energy and order by employing two polynomial conditions on the HeunC function. Based on these findings, I obtain the relation between the real and imaginary values of energy [11-17]. In the last section, I calculate the changes in stability time with mass for different values of polynomial order (N) [18,19,20]. Furthermore, I present the relationship between time of a stable orbit and N graphically.

2. Stable Bound States

The four-dimensional Klein Gordon (KG) equation can be written as

$$(\Box + m^2)\psi = 0 \tag{2.1}$$

Where, $\Box_g = \frac{1}{\sqrt{g}}\frac{\partial}{\partial x^\mu}\sqrt{g}g^{\mu\nu}\frac{\partial}{\partial x^\nu}$ is the d'Almebert operator in the general coordinate system. Now, using the Schwarzschild metric in equation (2.1) gives to the differential equation of the form

$$\frac{-r^2}{(1-\frac{1}{r})}\frac{\partial^2\psi}{\partial t^2} + \frac{\partial}{\partial r}(r^2 - r)\frac{\partial\psi}{\partial r} + \frac{1}{\sin\theta}\frac{\partial}{\partial\theta}(\sin\theta\frac{\partial\psi}{\partial\theta}) + \frac{\partial^2\psi}{\partial\phi^2} + m^2 r^2\psi = 0 \tag{2.2}$$

For our case, since spin is zero for scalar particle, so last term that contain spin is taken as zero. Then, the total solution of equation (2.2) read as

$$\psi(t,r,\theta) = \exp^{-iwt} R(r)P_l(\cos\theta) \tag{2.3}$$

Exponential term of above equation is time part T = $\exp^{-iwt}$, second is radial and third is angular solution. Now, Using equation (2.3) into (2.2) gives,

$$\frac{\partial}{\partial r}(r^2 - r)\frac{\partial R(r)}{\partial r} + (w^2 - (1 - \frac{1}{r})(\frac{l^2}{r^2} + m^2))R(r) = 0 \tag{2.4}$$

This is important equation for calculation of numerous phenomena. From (2.4), it is clear that solution of it depends on mass of an object, energy of massive particle, angular momentum and distance from Schwarzschild black hole.

Now, to obtain potential energy, (2.4) should be converted into Schrodinger equation because of presence of first order derivatives in it. For this, I have used tortoise coordinate i.e.

$$r^* = r + \ln(r - 1) \tag{2.5}$$

Using equation (2.5) into equation (2.4) and taking the symmetric wave function,
i.e., $R(r) = \frac{\phi(r)}{r}$ gives

$$\frac{d^2\Phi(r*)}{dr^{*2}} + [w^2 - V(r)]\Phi(r^*) = 0 \tag{2.6}$$

Where,

$$V(r) = (1 - \frac{1}{r})(\frac{l(l+1)}{r^2} + \frac{1}{r^3} + m^2) \tag{2.7}$$

This is the potential energy of scalar particle. Nature of it is depends on mass, distance from event horizon and angular momentum. The result is different than classical approach [21]. Because, potential energy from classical way is

$V(r) = (1 - \frac{1}{r})(1 + \frac{l^2}{r^2})$. So, phenomena than classical approach can be expected

for scalar particle from (2.6). Here, to evaluate dynamics of stable orbit, we have to differentiate (2.7) with respect to r and equates it to zero [22]. Which gives

$$m = \frac{\sqrt{-4 + 3r - 3rl + 2r^2l - 3rl^2 + 2r^2l^2}}{r^{\frac{3}{2}}} \tag{2.8}$$

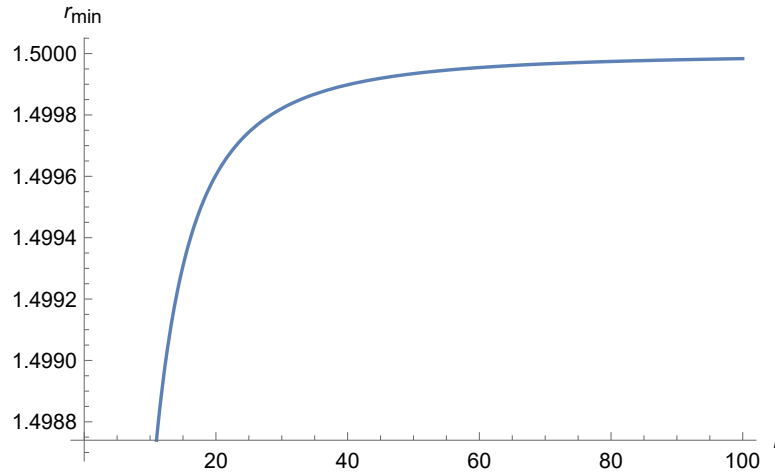Since $m > 0$, one of the solution of (2.8) gives

Figure 1: Relation between minimum r and l for stable orbit

From above figure, it is clear that at l=0, minimum stable orbital distance from Schwarzschild black hole is 1.34 and its value increases gradually up to about 1.49 and nearly become constant with increase in l. Below this value for particular l, stable orbit doesn't exist at all. Similarly, near the Schwarzschild black hole, the relation between mass and distance is obtained for particular l from (2.8) which is shown in below figure
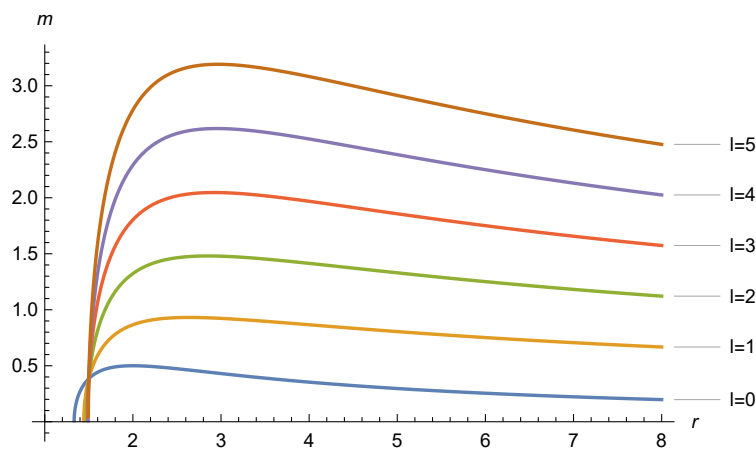

Figure 2: Relation between mass for stable orbit and its distance near Schawarzschild black hole

From this figure, it can be said that ,for any value of l, mass carried by scalar particle for stable orbit is initially increase with increased in r and decreases with increasing r. The highest value of mass in stable orbit is called maximum mass (m_{max}). Stable orbit for m_{max} is increased with increase in angular momentum is tabulated below

l	m_{max}	r
0	0.487637	1.79926
1	0.921105	2.40411
2	1.48206	2.73894
3	2.06002	2.84695
4	2.62098	2.87935
5	3.19894	2.91175

The outcome presented in the table contradicts Newton's theory of gravitation. According to Newton's theory , lighter objects should revolve around heavier masses. However, the table's findings demonstrate that even when a weaker gravitational field possesses a greater mass, the revolution of particles around a stronger gravitational field occurs. In this case, the stronger field represents a black hole, while other fields with greater, equal, or lesser masses than the black hole are considered weaker in comparison. This phenomenon suggests that the strength of the gravitational field has a greater impact than the mass itself. As a result, this serves as

a notable example of the successful application of the General Theory of Relativity. Beyond this mass for given l, no stable orbit is existed. Similarly, far from the Schwarzschild black hole, the relation between mass and distance is obtained from (2.8) which is shown in below figure.
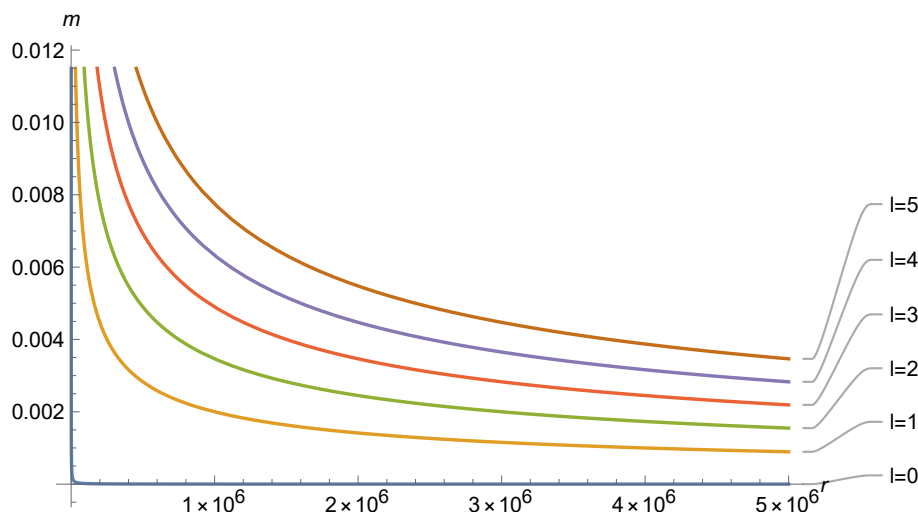

Figure 3: Relation between mass of stable orbit and distance far from Schawarzschild black hole.

From above figure, it can be said that smaller mass can make stable orbit far from Schwarzschild black hole and vice versa.

3. Quasi Normal Modes
Due to strong gravity of Schwarzschild black hole, orbit has certain time of stability. After that, it will leave the path. This causes complex value of energy which is called quasi normal modes. In order to obtain it, we have to solve (2.4).

The general solution of (2.4) is

$$R(r) = C_1 (r-1)^{iw} e^{-\sqrt{m^2 - w^2}\, r} HeunC\left(2\sqrt{m^2 - w^2}, 2\,iw, 0, m^2 - 2\,w^2, -l^2 - \delta, -r+1\right) +$$
$$C_2 (r-1)^{-iw} e^{\sqrt{m^2 - w^2}\, r} HeunC\left(-2\sqrt{m^2 - w^2}, -2\,iw, 0, m^2 - 2\,w^2, -l^2 - \delta, -r+1\right)$$

(3.1)

where $\delta = m^2 - 2w^2$.

It is the general Heun polynomial solution for the scalar particle containing confluent Heun function (HeunC). First part of this solution is for in going, while second part is for outgoing particle. HeunC can be expanded for N order by using two polynomial conditions and these conditions give specific energy for given mass of stable orbit. Two polynomial conditions are

$$\frac{\delta}{\alpha} + \frac{\beta + \gamma}{2} + N + 1 = 0$$

(3.2)

And

$$\Delta_{N+1}(\mu) = 0$$

(3.3)

Here, integer $N \geqslant 0$ is order of polynomial and $\Delta_{N+1}(\mu)$ is determinant of three diagonal matrix. Equation (3.2) is called δ_n condition. This is obtained when we take $C_0 = 0$ and $n = N$. Similarly, equation(3.3) gives $c_{n+1} = 0$. The power series being cut after its Nth term when it full fill both conditions and thus gives the polynomial solution [23-25]. General form of Heun solution for scalar particle is of the form:

$$H(z) = C_1 HeunC(\alpha, \beta, \gamma, \delta, \eta, z) + C_2 z^{-\beta} HeunC(\alpha, -\beta, \gamma, \delta, \eta, z)$$

(3.4)

Comparing HeunC of equation (3.4) with (3.1), we get the parameter inside the HeunC and using it in equation (3.2) and (3.3) gives energy for specific value of mass and polynomial order (N). For different value of m, variation of energy (w) with N is tabulated below

S.N.	m	N=0	N=1	N=2
		w_0	w_1	w_2
1	0.9	$\pm0.8795017033990309 + 0.0416912295931$ i	$\pm0.8872202331236642 + 0.01162276185780027$ i	$\pm0.8924915037509322 + 0.004506614821280622$ i
2	0.8	$\pm0.782354789947242 + 0.030759405778067$ i	$\pm0.7901099686647353 + 0.007958116126735462$ i	$\pm0.7944265108020128 + 0.002970999818233123$ i
3	0.7	$\pm0.685501164599239 + 0.021471189234520$ i	$\pm0.692724806366438 + 0.005105266948209186$ i	$\pm0.696068460546929 + 0.001832925693875396$ i
4	0.6	$\pm0.5887997114766707 + 0.01389403215343$ i	$\pm0.5949943358339548 + 0.0030044098808537645$ i	$\pm0.597404692817181 + 0.0010369529380656116$ i
5	0.5	$\pm0.49206361205258325 + 0.0080687141373$ i	$\pm0.49685676012059304 + 0.0015703790969961433$ i	$\pm0.498433905850676 + 0.0005214857802321435$ i
6	0.4	$\pm0.39505498433236763 + 0.0039790580634$ i	$\pm0.39826979521145406 + 0.0006913019587104053$ i	$\pm0.39916898744749285 + 0.00022142218116341227$ i
7	0.3	$\pm0.2974971679169774 + 0.00150220494043$ i	$\pm0.29922452461641064 + 0.00023242296469331046$ i	$\pm0.2996391653908074 + 0.00007212872385291664$ i
8	0.2	$\pm0.19913489760572703 + 0.0003456509794$ i	$\pm0.19975944359387166 + 0.0000480858159019386$ i	$\pm0.1998907973066362 + 0.000014556595933645497$ i
9	0.1	$\pm0.09987972179693583 + 0.000024042908$ i	$\pm0.09996905438224099 + 0.000003094097320442027$ i	$\pm0.09998617158915306 + 9.218311645906113 \times 10^{-7}$ i
10	0.09	$\pm0.08991168480085794 + 0.0000158896937$ i	$\pm0.08997739884418397 + 0.000002033854822175608$ i	$\pm0.08998991074361375 + 6.053218185603564 \times 10^{-7}$ i
11	0.08	$\pm0.07993757015340408 + 0.0000099851771$ i	$\pm0.0799841001187318 + 0.000001271866524815349$ i	$\pm0.07999290873994104 + 3.781839175125361 \times 10^{-7}$ i
12	0.07	$\pm0.06995793535714132 + 0.0000058873846$ i	$\pm0.06989933268322005 + 7.466561150185039 \times 10^{-7}$ i	$\pm0.06999524630009456 + 2.218318455770368 \times 10^{-7}$ i
13	0.06	$\pm0.0599733769587725 + 0.00000319408677$ i	$\pm0.059993273829075836 + 4.035478790401217 \times 10^{-7}$ i	$\pm0.05999700471697138 + 1.198083449257831 \times 10^{-7}$ i
14	0.05	$\pm0.049984527191120495 + 0.000001547049$ i	$\pm0.04999610333754176 + 1.948255878592198 \times 10^{-7}$ i	$\pm0.049998265785518484 + 5.780615022562324 \times 10^{-8}$ i
15	0.04	$\pm0.0399920500593659 + 6.35933262 \times 10^{-7}$ i	$\pm0.03999800314464758 + 7.98722299506466 \times 10^{-8}$ i	$\pm0.03999911173286294 + 2.368686120984056 \times 10^{-8}$ i
16	0.03	$\pm0.029996636914537918 + 2.017739 \times 10^{-7}$ i	$\pm0.029999156996794715 + 2.528974179074199 \times 10^{-8}$ i	$\pm0.02999962514759344 + 7.497001349317739 \times 10^{-9}$ i
17	0.02	$\pm0.01999900157232379 + 3.9936115 \times 10^{-8}$ i	$\pm0.019999750098395625 + 4.998000899550637 \times 10^{-9}$ i	$\pm0.019999888908329655 + 1.481218159680231 \times 10^{-9}$ i
18	0.01	$\pm0.009999875049197813 + 2.4990005 \times 10^{-9}$ i	$\pm0.009999968753075844 + 3.1246875351867 \times 10^{-11}$ i	$\pm0.00999998611171872 + 9.258847758135722 \times 10^{-11}$ i
19	0.009	$\pm0.008999908904053165 + 1.6397188 \times 10^{-9}$ i	$\pm0.008999977220566292 + 2.050146439825544 \times 10^{-11}$ i	$\pm0.00899998987535879 + 6.074781309465326 \times 10^{-11}$ i

S.N.	m	N=3	N=4	N=5
		w_3	w_4	w_5
1	0.9	$\pm0.895241930097688 + 0.002138902827721407$ i	$\pm0.896764309602307 + 0.001163566937510369$ i	$\pm0.8976735738492317 + 0.000697268894079972$ i
2	0.8	$\pm0.7965395904229081 + 0.0013826039174208106$ i	$\pm0.7976729377850408 + 0.0007439089053521748$ i	$\pm0.7983379748949857 + 0.00044284436232682454$ i
3	0.7	$\pm0.6976065962593437 + 0.000836784369924551$ i	$\pm0.6984072425343247 + 0.00044558384209638014$ i	$\pm0.6988693808476578 + 0.0002636328367382062$ i
4	0.6	$\pm0.5984490492328213 + 0.0004648459293866209$ i	$\pm0.5989777204928309 + 0.00024517413685685204$ i	$\pm0.5992783307816149 + 0.00014425744770583327$ i
5	0.5	$\pm0.4990797962701947 + 0.00022987887194706624$ i	$\pm0.49939860898467914 + 0.0001202145397548547$ i	$\pm0.49957750049577815 + 0.00007038931039264138$ i
6	0.4	$\pm0.3995188871877433 + 0.0000961716318038772$ i	$\pm0.39968785076702035 + 0.0000499258854044686784$ i	$\pm0.3997815946132724 + 0.000029113191867290994$ i
7	0.3	$\pm0.29979362547298954 + 0.00003094624969315101$ i	$\pm0.29986688479386253 + 0.00001597043383779796$ i	$\pm0.299907163146723 + 0.000009282291961325766$ i
8	0.2	$\pm0.19993810876448198 + 0.000006188194640884055$ i	$\pm0.1999602502968295 + 0.000003179666312039719$ i	$\pm0.19997234317830612 + 0.0000018436623291 81222$ i
9	0.1	$\pm0.09999220667508352 + 3.896511757184396 \times 10^{-7}$ i	$\pm0.09999500786161895 + 1.996805748767781 \times 10^{-7}$ i	$\pm0.09999653157103697 + 1.156123004512464 \times 10^{-7}$ i
10	0.09	$\pm0.08999431601590228 + 2.557712565437836 \times 10^{-7}$ i	$\pm0.08999635964370636 + 1.310501864371189 \times 10^{-7}$ i	$\pm0.08999747099038415 + 7.586922537239401 \times 10^{-8}$ i

11	0.08	± 0.07999600628929517 $+ 1.597444599012932 \times 10^{-7}$ i	± 0.0799974425776719 $+ 8.183621043601788 \times 10^{-8}$ i	± 0.07999822346572588 $+ 4.737372241968112 \times 10^{-8}$ i
12	0.07	± 0.0699973235396207 $+ 9.367432899726962 \times 10^{-8}$ i	± 0.06999828632244821 $+ 4.798238549356557 \times 10^{-8}$ i	± 0.06999880966569494 $+ 2.777423135469184 \times 10^{-8}$ i
13	0.06	± 0.05999831399358943 $+ 5.057948358148399 \times 10^{-8}$ i	± 0.05999892061198497 $+ 2.590507974780383 \times 10^{-8}$ i	± 0.05999925029518688 $+ 1.499400269863547 \times 10^{-8}$ i
14	0.05	± 0.049999024037915576 $+ 2.439881443173898 \times 10^{-8}$ i	± 0.04999937524598907 $+ 1.249500224886014 \times 10^{-8}$ i	± 0.04999956609086663 $+ 7.231787536181143 \times 10^{-9}$ i
15	0.04	± 0.03999950019679125 $+ 9.996001799101276 \times 10^{-9}$ i	± 0.039999680080618036 $+ 5.118689657449965 \times 10^{-9}$ i	± 0.04999956609086663 $+ 7.231787536181143 \times 10^{-9}$ i
16	0.03	± 0.02999978910920818 $+ 3.163350766098319 \times 10^{-9}$ i	± 0.029999865019133317 $+ 1.619766757799259 \times 10^{-9}$ i	± 0.02999990625922753 $+ 9.374062605733485 \times 10^{-10}$ i
17	0.02	± 0.01999993750615169 $+ 6.249375070373587 \times 10^{-10}$ i	± 0.01999996000251983 $+ 3.199795214850327 \times 10^{-10}$ i	± 0.01999997222343744 $+ 1.851769551627144 \times 10^{-10}$ i
18	0.01	± 0.009999992187692257 $+ 3.906152346317094 \times 10^{-11}$ i	± 0.009999995000078747 $+ 1.999968001222837 \times 10^{-11}$ i	± 0.009999996527815753 $+ 1.15739454801745 \times 10^{-11}$ i
19	0.009	± 0.008999994304801025 $+ 2.562838727807545 \times 10^{-11}$ i	± 0.0089999963550465 $+ 1.312182994170376 \times 10^{-11}$ i	± 0.008999997468772425 $+ 7.593681657639989 \times 10^{-12}$ i

Numerical calculations provide that real value of energy carry both positive and negative with equal magnitude while imaginary parts carry only positive value. Furthermore, with decreasing mass and increasing N, imaginary parts become smaller. For different value of N, real and imaginary values of energy are given below
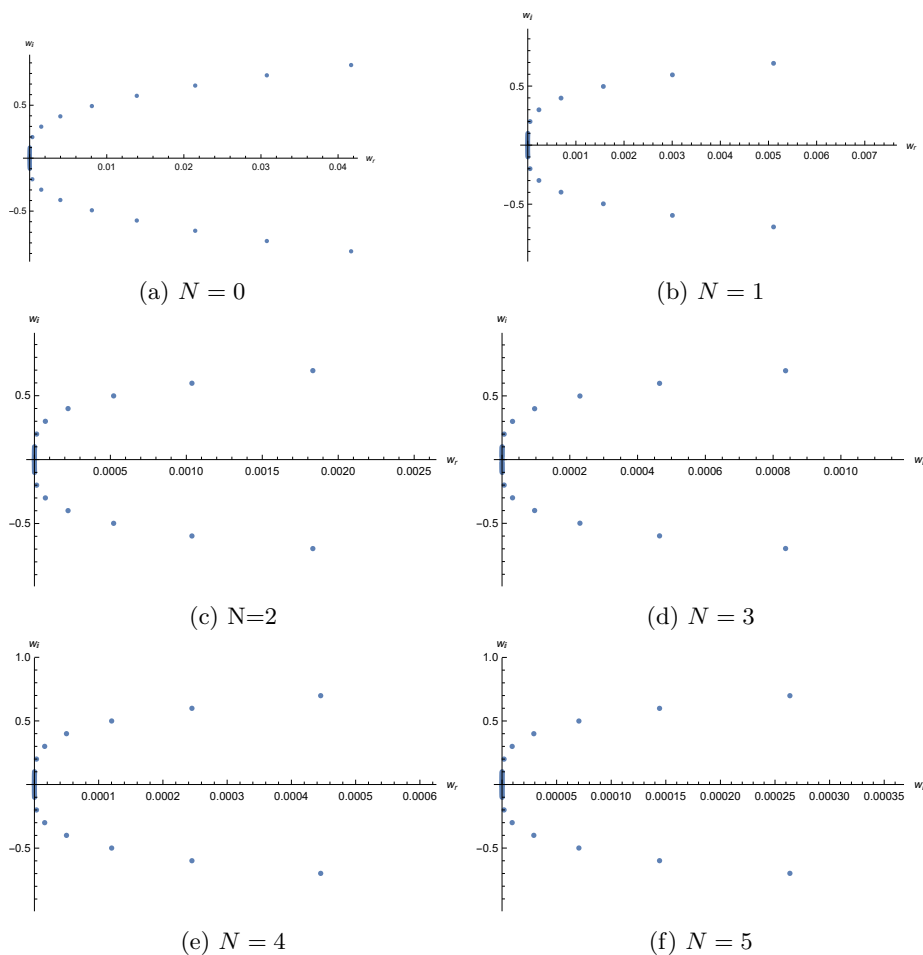

(a) $N = 0$

(b) $N = 1$

(c) N=2

(d) $N = 3$

(e) $N = 4$

(f) $N = 5$

Figure 4: Relation between imaginary and real value of energy for given N
Parabolic relation between real and imaginary value of energy for any N can be easily seen for different m.

4. Stability of Orbit

From quasi normal modes in previous section, we get energy of the form $w = a + ib$. Using this value in $\exp^{-iwt}$ of (2.3) gives

$$T = \exp^{ia} exp^{-bt} \qquad (4.1)$$

First term of (4.1) gives nature of in coming particle. While second term gives decay rates and reciprocal of it provides time for stable orbit[7, 26]. Using this concept on table of quasi normal modes give
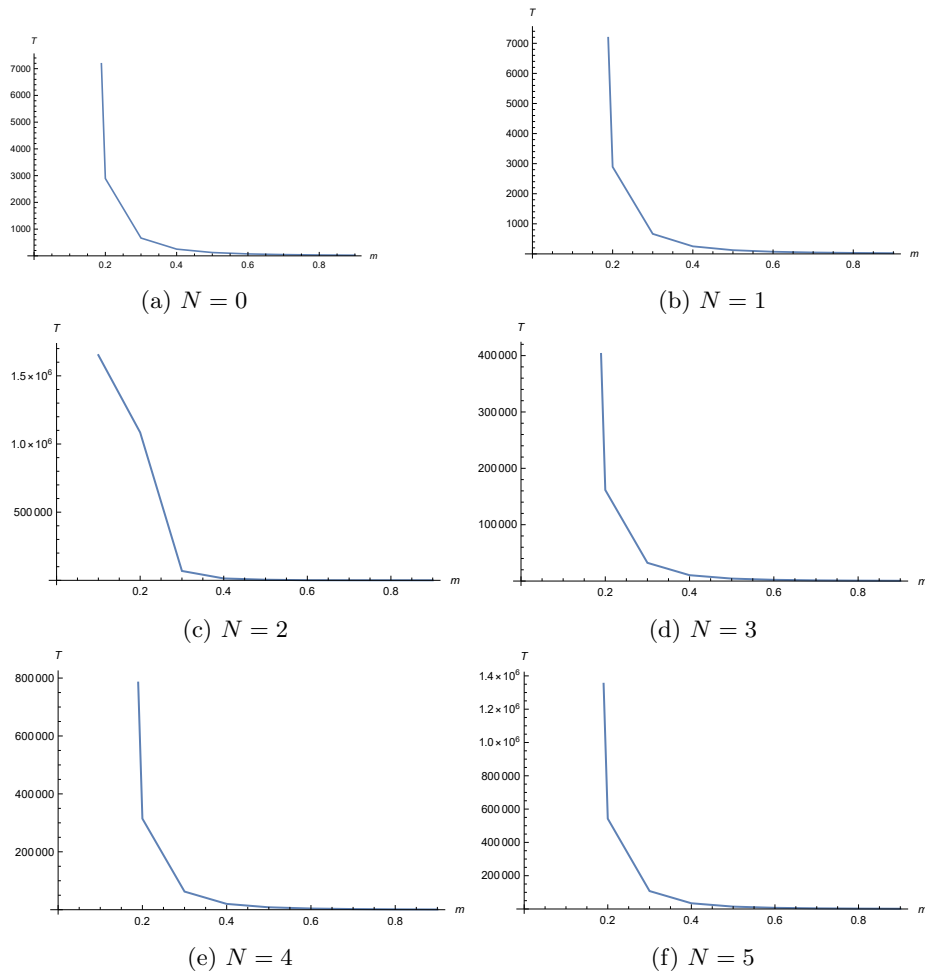

Figure 5: Relation between time of stability and mass

Above six figures tell us that with decrease in mass, the stability is increased and vice versa. Which means m is inversely proportional to stability time. From figure (2) and (3), mass for stable orbit is inversely proportional to distance. Combining this idea, and using figure (2), (3) and (5), it can be said that stability of orbit decreased up to m_max and then increases rapidly as distance from Schwarzschild black hole is increased. In other word, near the Schwarzschild black hole, due to very strong gravity, its stability is decreased and far from black hole cause long revolution of smaller mass. Again, for same m
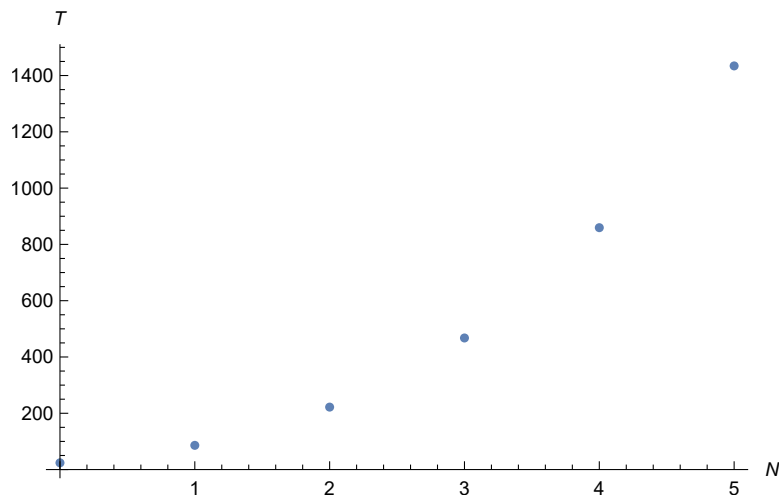
Figure 6: Relation between T and N for m=0.9

From figure (6), it is also clear that with increase in polynomial order, stability of orbit is increased. Therefore, expansion of HeunC up to larger value of N can provides much accurate information about orbital stability and its energy.

5. Discussion and Conclusion

In the second section of my work, I derived the potential energy for scalar particles based on the massive Klein-Gordon field. This energy formula is applicable to scalar particles such as mesons or smaller particles. It can also be applied to celestial bodies like planets and stars. The obtained potential energy was different from that of classical approximations. Therefore, it provides a more accurate analysis of the dynamics of scalar particles. Consequently, the relationship between the mass of a body, its angular momentum, and its distance near the Schwarzschild black hole was correctly explained. This result challenges the traditional concept of independence of mass. As we move away from the Schwarzschild black hole, the mass required for stability initially increases and then decreases after reaching a peak value. This can be attributed to larger masses being able to sustain revolution near the black hole for a certain period. The mass of a revolving object can be greater than that of the black hole itself. However, Newtonian theory predicts the revolution of a lighter body around a heavier one. The contrasting result from this section tells us that the strong gravity of the black hole is the cause rather than its mass. As we move farther from the black hole, the gravitational force weakens, allowing smaller particles to revolve around it. In the third section, I applied polynomial conditions to the HeunC function. This approach resulted in obtaining the energy for different values of N and m. Unlike classical and quantum mechanical predictions, the energy obtained through this method has a complex nature, known as quasi-normal modes. The real part of the energy has both positive and negative values with the same magnitude, while the imaginary part is always positive. For any value of N, the plot between real and imaginary values follows a parabolic pattern. Furthermore, the real value of energy is nearly equal to the mass of an object, while the imaginary value decreases as N is increased and m is decreased. In the last section, I utilized the calculations from the second and third sections to determine the stability time for orbital motion. This has an inverse relationship with the imaginary energy. By performing mathematical calculations based on the results obtained in the previous sections, I found that the stability time of bound states near the Schwarzschild black hole decreases for heavier masses due to the strong gravitational field. Therefore, heavier objects have a shorter survival time. However, as we move farther from the black hole, the orbital motion of smaller masses becomes possible, resulting in longer stability times. This is because the gravitational field is weaker in that region. This effect is clearly observed in the calculations presented in this section. Again, keeping distance and polynomial order constant, the mass of a scalar object is inversely proportional to the time period. It means that a larger mass will have a shorter lifespan in these paths. This concept can be used in the motion of artificial satellites near Earth with greater accuracy. Moreover, with an increase in polynomial order, the stability time for the same mass increases. A larger expansion of the function leads to greater accuracy in orbital motion. Therefore, in addition to the research conducted in this study, other dynamical properties of the Klein-Gordon equation, such as scattering and probability density, can be calculated by considering a larger expansion of these functions.

References

1. Gui-hua, T., Wang, S. K., & Zhong, S. (2006). The effect of the tortoise coordinate on the stable study of the Schwarzschild black hole. arXiv preprint gr-qc/0603113.
2. Tian, G. H., Wang, S. K., & Zhong, S. (2006). The tortoise coordinates and the cauchy problem in the stable study of the Schwarzschild black hole. arXiv preprint gr-qc/0608044.
3. Philipp, D., & Perlick, V. (2015). On analytic solutions of wave equations in regular coordinate systems on Schwarzschild background. arXiv preprint arXiv:1503.08101.
4. Konoplya, R. A., & Abdalla, E. (2005). Scalar field perturbations of the Schwarzschild black hole in the Gödel universe.

Physical Review D, 71(8), 084015.

5. Koyama, H., & Tomimatsu, A. (2001). Asymptotic tails of massive scalar fields in a Schwarzschild background. Physical Review D, 64(4), 044014.

6. Wald, R. M. (1994). Quantum field theory in curved spacetime and black hole thermodynamics. University of Chicago press.

7. Konoplya, R. A., & Zhidenko, A. V. (2005). Decay of massive scalar field in a Schwarzschild background. Physics Letters B, 609(3-4), 377-384.

8. Konoplya, R. A., & Zhidenko, A. (2011). Quasinormal modes of black holes: From astrophysics to string theory. Reviews of Modern Physics, 83(3), 793.

9. Bhattacharyya, M. K., Hilditch, D., Nayak, K. R., Rüter, H. R., & Brügmann, B. (2020). Analytical and numerical treatment of perturbed black holes in horizon-penetrating coordinates. Physical Review D, 102(2), 024039.

10. Li, W. D., Chen, Y. Z., & Dai, W. S. (2019). Scattering state and bound state of scalar field in Schwarzschild spacetime: Exact solution. Annals of Physics, 409, 167919.

11. Övgün, A., Sakallı, I., & Saavedra, J. (2018). Quasinormal modes of a Schwarzschild black hole immersed in an electromagnetic universe. Chinese Physics C, 42(10), 105102.

12. Barranco, J., Bernal, A., Degollado, J. C., Diez-Tejedor, A., Megevand, M., Alcubierre, M., ... & Sarbach, O. (2014). Schwarzschild scalar wigs: spectral analysis and late time behavior. Physical Review D, 89(8), 083006.

13. Rosa, J. G., & Dolan, S. R. (2012). Massive vector fields on the Schwarzschild spacetime: quasinormal modes and bound states. Physical Review D, 85(4), 044043.

14. Giri, S., Nandan, H., Joshi, L. K., & Maharaj, S. D. (2022). Geodesic stability and quasinormal modes of non-commutative Schwarzschild black hole employing Lyapunov exponent. The European Physical Journal Plus, 137(2), 1-11.

15. Bezerra, V. B., Christiansen, H. R., Cunha, M. S., & Muniz, C. R. (2017). Exact solutions and phenomenological constraints from massive scalars in a gravity's rainbow spacetime. Physical Review D, 96(2), 024018.

16. Bhattacharyya, M. K., Hilditch, D., Nayak, K. R., Rüter, H. R., & Brügmann, B. (2020). Analytical and numerical treatment of perturbed black holes in horizon-penetrating coordinates. Physical Review D, 102(2), 024039.

17. Fiziev, P., & Staicova, D. (2011). Application of the confluent Heun functions for finding the quasinormal modes of nonrotating black holes. Physical Review D, 84(12), 127502.

18. Fiziev, P. P. (2009). Novel relations and new properties of confluent Heun's functions and their derivatives of arbitrary order. Journal of Physics A: Mathematical and Theoretical, 43(3), 035203.

19. Fiziev, P., & Staicova, D. (2012, July). Solving systems of transcendental equations involving the Heun functions. In AIP Conference Proceedings (Vol. 1458, No. 1, pp. 395-398). American Institute of Physics.

20. Fiziev, P. P. (2009). Classes of exact solutions to Regge-Wheeler and Teukolsky equations. arXiv preprint arXiv:0902.1277.

21. Chandrasekhar, S., & Thorne, K. S. (1985). The mathematical theory of black holes.

22. Goldstein, H., Poole, C., & Safko, J. (2002). Classical mechanics.

23. Giscard, P. L., & Tamar, A. (2022). Elementary integral series for Heun functions: Application to black-hole perturbation theory. Journal of Mathematical Physics, 63(6).

24. Birkandan, T., & Hortaçsu, M. (2017). Quantum field theory applications of Heun type functions. Reports on Mathematical Physics, 79(1), 81-87.

25. Vieira, H. S., & Bezerra, V. B. (2016). Confluent Heun functions and the physics of black holes: Resonant frequencies, Hawking radiation and scattering of scalar waves. Annals of Physics, 373, 28-42.

26. Lasenby, A., Doran, C., Pritchard, J., Caceres, A., & Dolan, S. (2005). Bound states and decay times of fermions in a Schwarzschild black hole background. Physical Review D, 72(10), 105014.